JOURNAL OF MATERIALS SCIENCE 26 (1991) 4110–4115

The intermediate compound in the In_2O_3–SnO_2 system

H. ENOKI, J. ECHIGOYA, H. SUTO*
Department of Materials Processing, Faculty of Engineering, Tohoku University, Sendai 980, Japan

The In_2O_3–SnO_2 binary system between 1473 and 1873 K has been investigated by TEM observations in detail. The intermediate compound has been detected above 1573 K in the composition range from 47.9 to 59.3 mol% SnO_2, that crystal structure is long range ordered cubic system similar to In_2O_3 phase. On the other hand, below 1473 K, the intermediate compound is decomposed into In_2O_3 and SnO_2 phases, according to the eutectoid reaction.

1. Introduction

Indium-tin-oxide (ITO) has found many applications, for example, in transparent electrodes for display devices, transparent coating for solar energy heat mirrors and window films in n-p heterojunction solar cells. Generally, ITO thin films are deposited by using several techniques [1–7] to control both composition and structure accurately, because the electrical and optical properties of ITO films strongly depend on not only heat treatment but also these compositions [1–3]. However, neither solubility nor phase diagram for the In–Sn–O system which is necessary to decide on the composition of films was reported in the past except for isothermal section of the In–Sn–O ternary phase diagram by G. Frank *et al.* [8] (see Fig. 1).

In the present work, the phase equilibria in the In_2O_3–SnO_2 pseudo-binary system at high temperature region from 1473 to 1873 K were determined using sintered specimens, and the solubility lines of each phase were clarified.

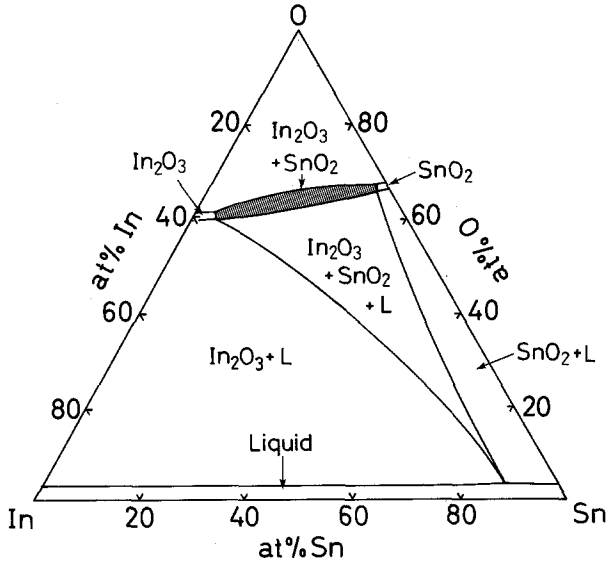

Figure 1 Isothermal section of the In–Sn–O ternary phase diagram at 873–1073 K by G. Frank *et al.* [8].

2. Experimental procedure

The specimens were prepared from In_2O_3 (99.97%) and SnO_2 (99.99%) powders by isostatic pressing. All of the specimens were heated at 1873 K for 36 ks in air for calcination, and equilibrated at fixed temperatures between 1473 and 1873 K for 360–1440 ks. The mean compositions of the specimens are shown in Table I. The decrease of SnO_2 after heating was due to evaporation of SnO_2, because the vapor pressure of the SnO_2 is higher than that of In_2O_3 [9].

The microstructures were observed by the transmission electron microscopy (TEM: JEOL JEM-200B) and scanning transmission electron microscopy (STEM: Hitachi H-800). The TEM and STEM specimens were prepared by ion beam thinning, after grinding until their thickness was 0.2 mm.

The chemical concentrations of In and Sn were determined by energy dispersion X-ray micro-analyser (EDX: Kevex 7500) equipped with STEM except for

TABLE I Specimen compositions

Treatment	The mean composition/mol % SnO_2 (χ_{Sn})	
	A	B
Isostatic pressing	50.0	70.0
	(33.3)	(53.8)
Calcination	48.2	65.7
(1873 K × 36 ks)	(31.8)	(48.9)
Isothermal ageing		
1873 K × 72 ks	45.9	62.1
	(29.8)	(45.0)
1673 K × 360 ks	46.9	64.2
	(30.6)	(47.3)
1573 K × 720 ks	47.9	64.7
	(31.4)	(47.8)
1473 K × 1440 ks	48.1	65.3
	(31.7)	(48.5)

* Now emeritus professor, Tohoku University.

0022–2461/91 $03.00 + .12

oxygen. The indications of the composition were molecular fraction of SnO_2 assuming that these are made up to the stoichiometric oxides, i.e. In_2O_3 or SnO_2, atomic fraction of Sn following:

$$\chi_{Sn} = \frac{C_{In}}{C_{In} + C_{Sn}} (\times 100\%)$$

where C_i is the atomic concentration of the ith element by EDX.

The lattice constants were measured by X-ray diffractometer (RIGAKU RAD-B) using nickel filtered CuK_α radiation.

3. Results

3.1. Microstructure

Fig. 2 shows the microstructure and electron diffraction patterns of In_2O_3–50 mol % SnO_2 at 1673 K for 360 ks. Two different phases; referred to as C_1 and C_2, can be seen for which C_1 was precipitated from the matrix (C_2). These microstructures were observed all of the temperature range from 1573 to 1873 K. According to the diffraction patterns, the C_1 phase is an In_2O_3-type ordered structure and the C_2 phase is a cubic structure with the lattice constants almost as the same of C_1. Moreover, the C_1 precipitates were coherent with the C_2 matrix. Perhaps, in the first place, only

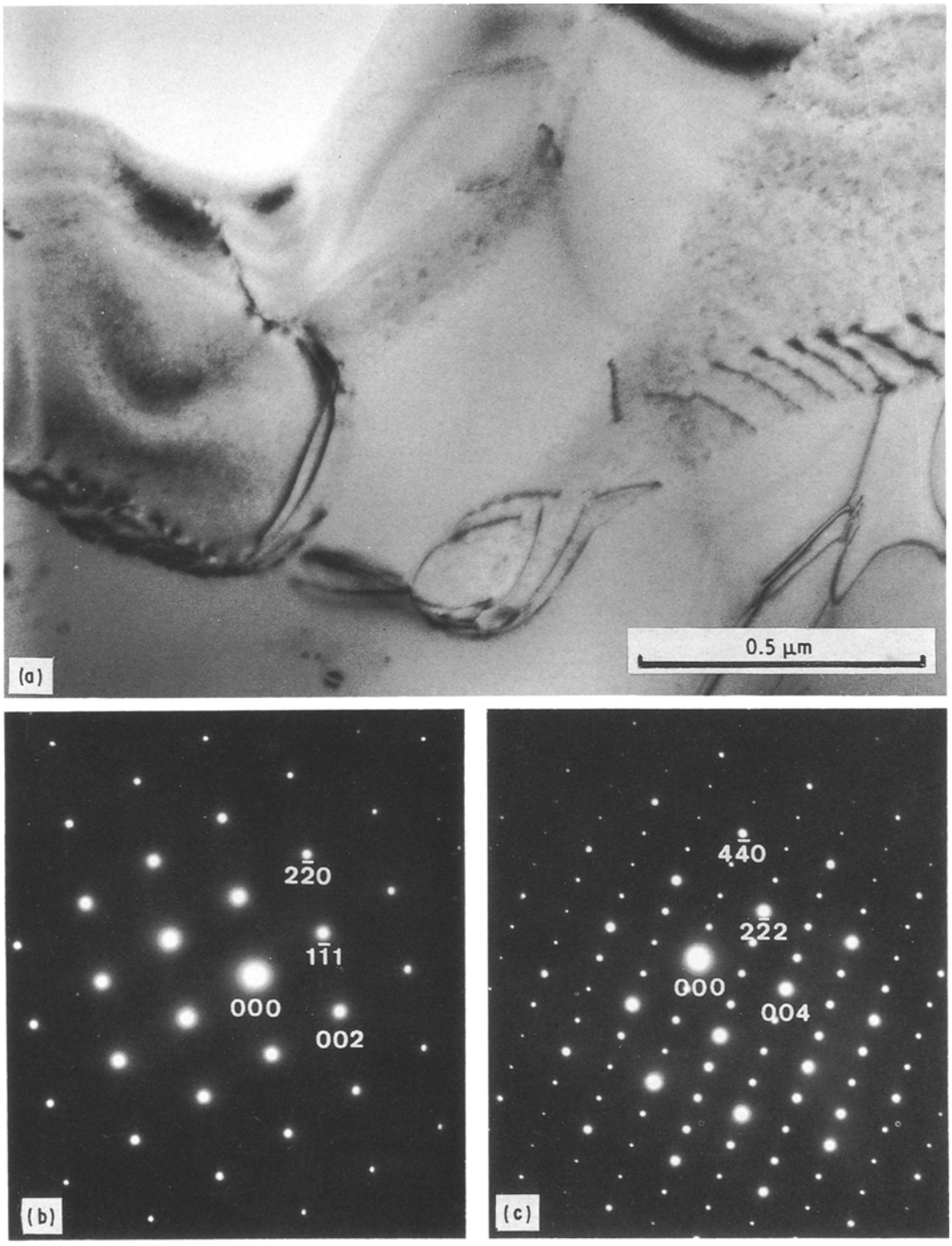

Figure 2 TEM photographs of In_2O_3–50 mol % SnO_2 at 1673 K for 360 ks. (a) Bright-field, (b) electron diffraction pattern of the matrix and (c) electron diffraction pattern of the precipitates.

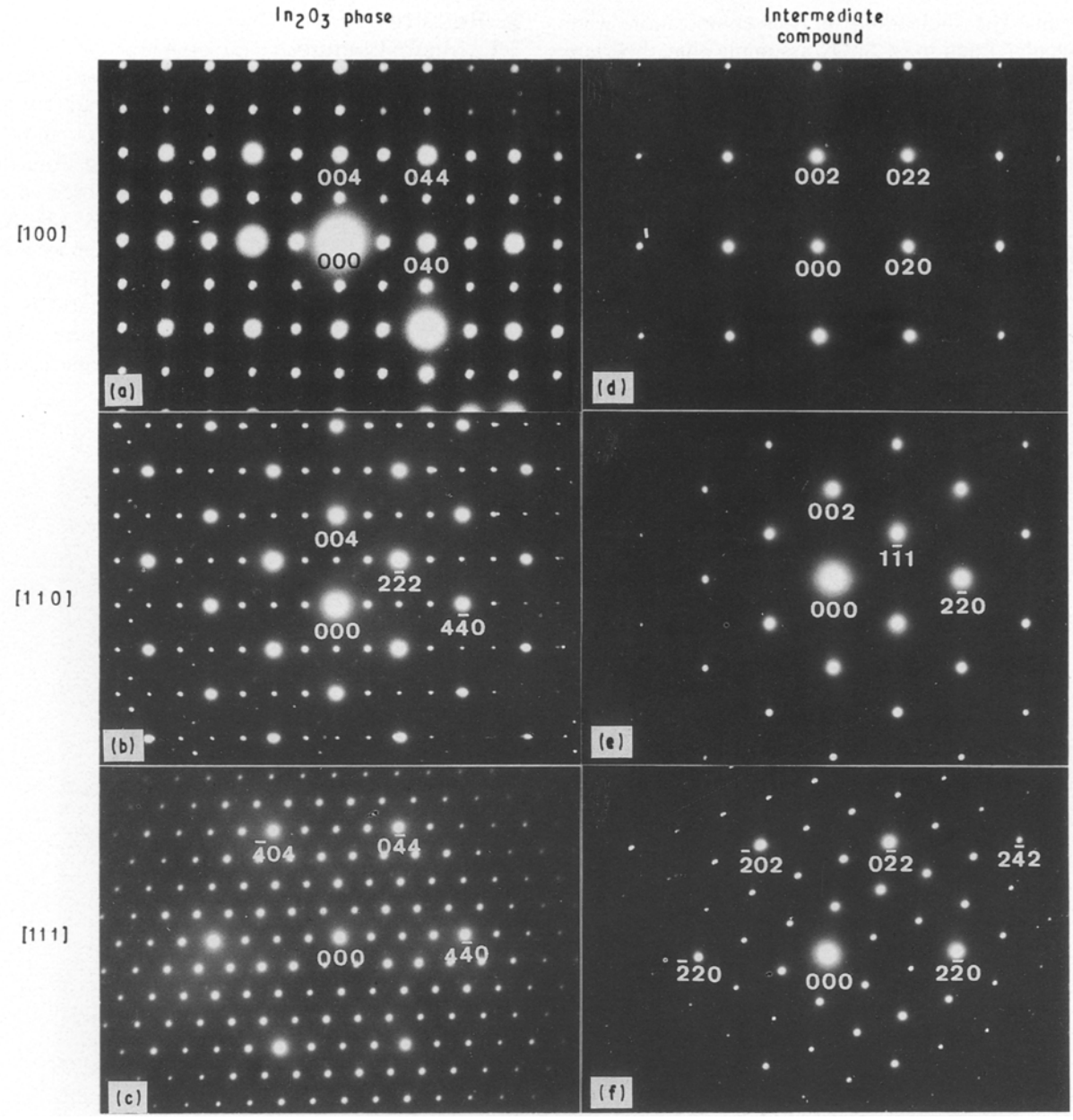

Figure 3 The electron diffraction patterns of (a) (b) (c) In_2O_3-phase (C_1) and (d) (e) (f) intermediate compound (C_2).

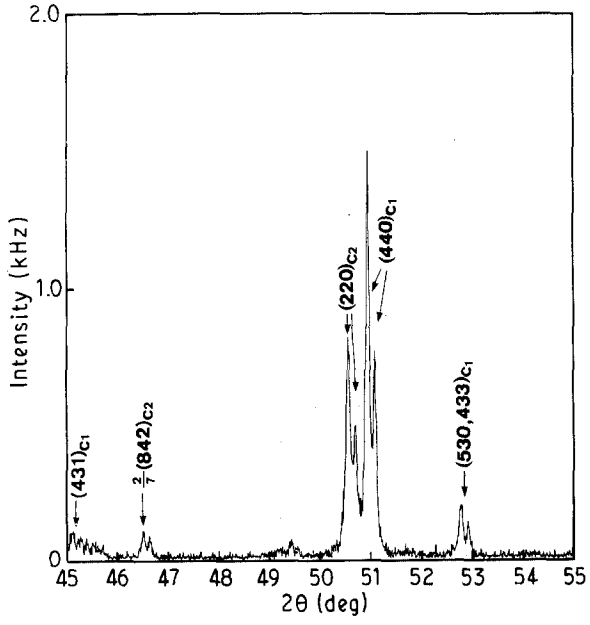

Figure 4 X-ray diffraction profiles obtained from In_2O_3–50 mol % SnO_2 at 1673 K for 360 ks.

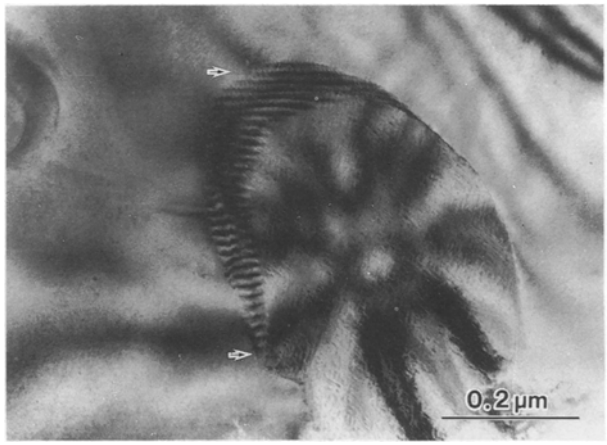

Figure 5 The misfit dislocation around the C_1 precipitate of In_2O_3–50 mol % SnO_2 at 1673 K for 360 ks.

the C_2 phase was formed at calcination, the mean composition became a (C_1 + C_2) two phase region during isothermal ageing, because of the decrease of SnO_2. Hence, the C_1 precipitates were coherent with

the C_2 matrix which have almost similar unit cell. The interface energy between C_1 and C_2 is independent of interface orientations because the shape of the C_1 precipitates is round. Fig. 3 shows the electron diffraction patterns for both In_2O_3 (C_1) and intermediate phase (C_2), respectively. The indices of the C_2 phase are based upon the C_1 phases. The In_2O_3 phase structure is an ordered cubic structure with a lattice parameter $a = 1.0118$ nm [10]. Comparing the C_1 and C_2 phases, similarities are noted in their fundamental structure. However, the extra reflections of C_2 only appeared when the diffraction pattern was taken from the [1 1 1] direction but without [1 0 0] and [1 1 0]. This suggests that the C_2 compound has a long range ordered cubic structure, although we did not analyse this structure in detail. The lattice parameters of these phases were measured in detail by X-ray diffractometry and are shown in Fig. 4. All of the fundamental reflections were split into two peaks. The lattice parameters of these phases were obtained: $a_{C1} = 1.012$ nm which is good agreement with the previous data, and $a_{C2} = 1.021$ nm respectively. From these results, the

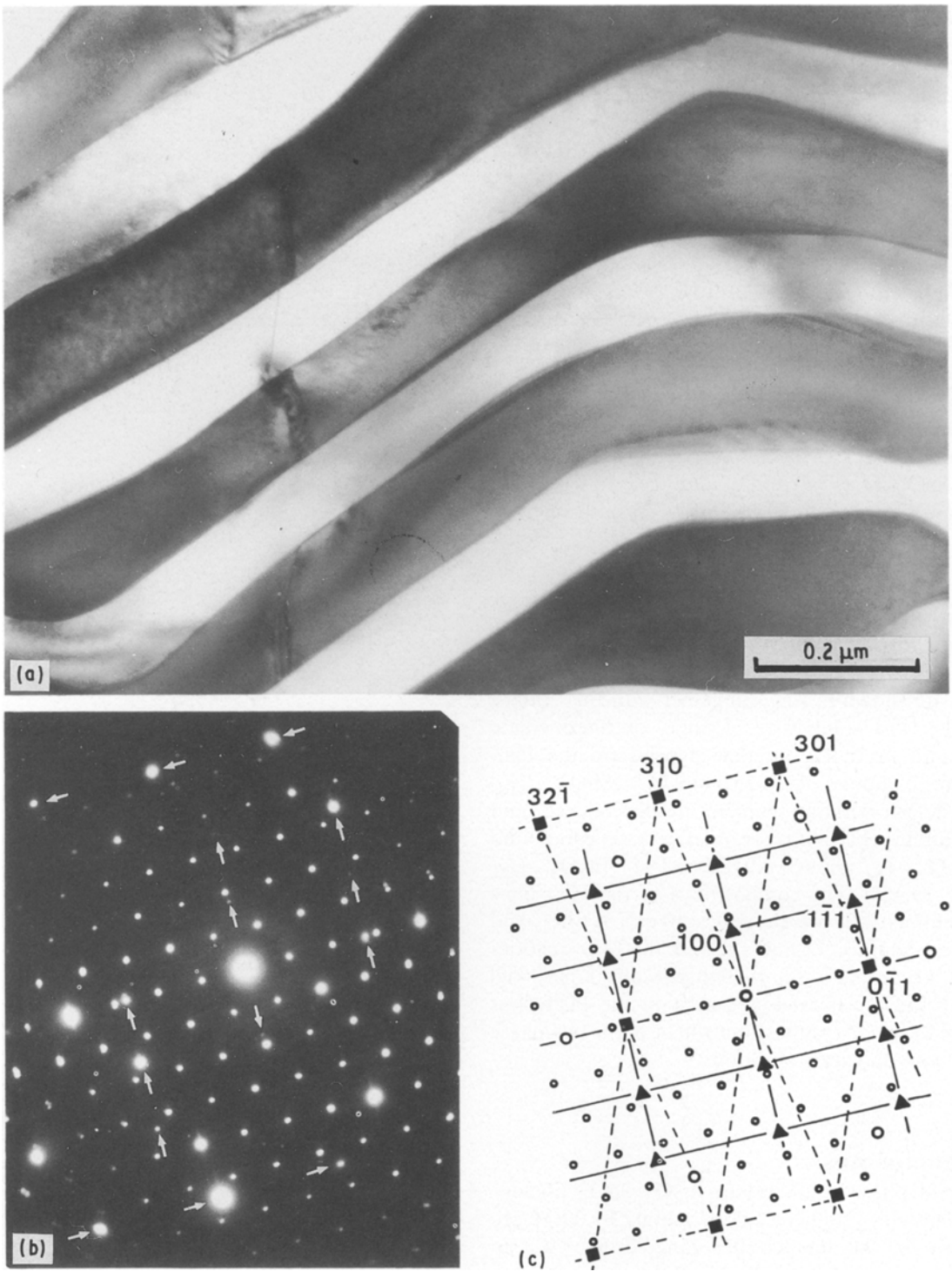

Figure 6 TEM photograph of In_2O_3–50 mol % SnO_2 at 1473 K for 1440 ks. (a) Bright-field, (b) electron diffraction pattern and (c) key diagram for (b). Open circles: In_2O_3 phase; triangles and squares: SnO_2 phase.

TABLE II Equilibrium composition

Temperature/K	Equilibrium composition/mol % SnO_2 (χ_{Sn})					
	C_1^a/C_2^a	C_2/C_1	C_2/T^a	T/C_2	C_1/T	T/C_1
1873	15.0 (8.1)	47.9 (31.5)	59.3 (42.1)	96.1 (92.5)	–	–
1673	19.8 (11.0)	56.9 (39.8)	58.5 (41.3)	94.8 (90.1)	–	–
1573	12.4 (6.6)	57.1 (40.0)	59.1 (41.8)	95.0 (90.4)	–	–
1473	–	–	–	–	15.0 (8.1)	94.4 (89.4)

[a] C_1; In_2O_3 phase, C_2; intermediate compound and T; SnO_2 phase.

lattice mismatch was calculated to be about 1%; the misfit dislocations at the interface were observed as shown in Fig. 5.

The microstructure of In_2O_3–50 mol % SnO_2 at 1473 K for 1440 ks is shown in Fig. 6. From the analysis of the electron diffraction patterns, the lamellar structures consisted of In_2O_3 (C_1) and SnO_2 (T) which is a rutile-type tetragonal structure for which $a = 0.4738$ nm, $c = 0.3188$ nm [11]. This means that the intermediate compound is not stable at 1473 K and so decomposed into these phases according to the eutectic reaction: $C_2 \rightleftarrows C_1 + T$. In this case, the orientation relationship between In_2O_3 and SnO_2 has two kinds of the crystallographic orientations at the interface. The (1 1 1) In_2O_3 plane is parallel to either (0 1 1) SnO_2 or (1 3 3) SnO_2 and the [1 1 0] In_2O_3 direction is parallel to [0 1 1] SnO_2 on both sides.

3.2. Equilibrium compositions

The equilibrium compositions of the In_2O_3–SnO_2 binary system are listed in Table II. The present results are shown in Fig. 7 together with the Frank's data [8]. The solubilities of SnO_2 or intermediate compound in In_2O_3 are few depend on the temperature about 12.4–15.0 mol % SnO_2 (χ_{Sn} = 6.6–8.1%) without temperature-dependence, and the solubility of In_2O_3 or intermediate compound in SnO_2 is about 3.9–5.6 mol % In_2O_3 (χ_{Sn} = 92.5–89.4%). The compositions of the ITO films used commercially are about 9 ~ 10 mol % SnO_2 and an excess addition of SnO_2 lowers the ITO qualities [3, 12]. According to the solubility results, it may well be that fine precipitates will exist in the ITO films because the mean composition will be in the two phase region with an excess addition.

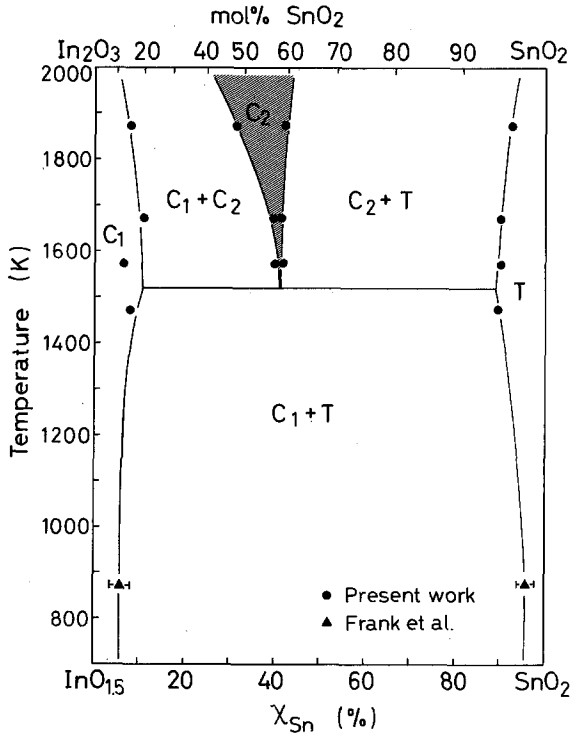

Figure 7 Summary of experimental results on phase equilibria in the In_2O_3–SnO_2 pseudo-binary system.

4. Conclusions

The solid phase equilibria in In_2O_3–SnO_2 pseudo-binary system were investigated mainly by TEM observation in the temperature range from 1473 to 1873 K.

1. The intermediate compound is formed in the composition range from 47.9 to 59.3 mol % SnO_2 above 1573 K. The crystal structure of this compound is an ordered cubic system.
2. Below 1473 K, the intermediate compound (C_2) was decomposed into both In_2O_3 (C_1) and rutile-type SnO_2 (T) phases according to the eutectoid reaction: $C_2 \rightleftarrows C_1 + T$.
3. The solubility of SnO_2 or intermediate compound in In_2O_3 is about 12.4 to 15.0 mol % SnO_2 without temperature-dependence. The value of the solubility is in good agreement with the composition of commercial ITO films. The solubility of In_2O_3 or intermediate compound in SnO_2 is about 96.1 to 94.4 mol % SnO_2 (3.9 to 5.6 mol % In_2O_3).

References

1. H. W. LEHMANN and R. WIDMER, *Thin Solid Films* **27** (1975) 359.
2. W. W. MOLZEN, *J. Vac. Sci. Technol.* **12** (1975) 99.

3. D. B. FRASER and H. D. COOK, *J. Electrochem. Soc.* **119** (1972) 1368.
4. F. H. GILLERY, *J. Vac. Sci. Technol.* **15** (1978) 306.
5. J. KANE, H. P. SCHWEITZER and W. KERN, *Thin Solid Films* **29** (1975) 155.
6. J. C. MANIFACIER, L. SZEPERSKI, J. F. BRESSE, M. PEROTIN and R. STUCK, *Mater. Res. Bull.* **13** (1978) 109.
7. R. GROTH, *Phys. Status Solidi* **14** (1966) 69.
8. G. FRANK, L. BROCK and H. D. BAUSEN, *J. Crst. Growth* **36** (1976) 179.
9. G. V. SAMSONOV (ed.),. "The Oxide Handbook Second Edition" (IFI/Plenum, New York, 1982).
10. Joint Committee on Powder Diffraction Standards (1978) 6-0416.
11. *Ibid.* (1971) 21–1250.
12. S. NOGUCHI and H. SAKATA, *Thin Solid Films* **157** (1988) 181.

Received 22 January
and accepted 30 November 1990